

Optical weights and waterfalls in doped charge-transfer insulators: A local density approximation and dynamical mean-field theory study of $\text{La}_{2-x}\text{Sr}_x\text{CuO}_4$

Cédric Weber, Kristjan Haule, and Gabriel Kotliar

Department of Physics, Rutgers University, Piscataway, New Jersey 08854, USA

(Received 25 August 2008; published 15 October 2008)

We use the local density approximation in combination with the dynamical mean-field theory to investigate intermediate energy properties of the copper oxides. We identify coherent and incoherent spectral features that result from doping a charge-transfer insulator, namely quasiparticles, Zhang-Rice singlet band, and the upper and lower Hubbard bands. Angle resolving these features, we identify a *waterfall*-like feature between the quasiparticle part and the incoherent part of the Zhang-Rice band. We investigate the asymmetry between particle and hole doping. On the hole-doped side, there is a very rapid transfer of spectral weight upon doping in the one particle spectra. The optical spectral weight increases superlinearly on the hole-doped side in agreement with experiments.

DOI: [10.1103/PhysRevB.78.134519](https://doi.org/10.1103/PhysRevB.78.134519)

PACS number(s): 74.20.-z, 71.10.-w, 71.27.+a, 74.25.-q

Since their discovery, the high temperature superconductors continue to be a subject of intensive investigations. It is widely believed that strong correlations and many-body effects are responsible for many of the peculiar properties of these materials. However, after many years of intensive studies, a comprehensive understanding of their electronic structure, even at intermediate energy scales, is lacking. The question of whether the strength of the on-site correlations is sufficient to open the gap at half filling (Mott picture) or alternatively magnetism is required (Slater picture) is actively debated.¹ A vertical feature in the photoemission spectral intensity, commonly known as a waterfall, has recently been found in many compounds,^{2,3} and it has been assigned to several conflicting microscopic origins.⁴⁻⁶

It is generally accepted that these materials contain copper-oxygen layers as a common element. Stoichiometric compounds, such as La_2CuO_4 , are antiferromagnetically ordered charge-transfer insulators in the Zaanen-Sawatsky-Allen^{7,8} classification scheme. Hence a minimal model of these materials contains two oxygen and one copper orbital per unit cell.⁹⁻¹¹

When this model is doped with electrons, the low energy physics is believed to be closer to that of the Hubbard model. On the hole-doped side, this reduction constructed by Zhang and Rice¹² can be achieved in the limit that the charge-transfer energy is much larger than the copper-oxygen hybridization. However, there is no agreement on the precise region (in energy and parameter space) where the reduction to a one-band model is accurate.

In this paper, we use a realistic theoretical approach, i.e., the local density approximation combined with the dynamical mean-field theory (LDA+DMFT),¹³ to study a typical cuprate compound $\text{La}_{2-x}\text{Sr}_x\text{CuO}_4$. The LDA calculation was done by PWSCF package,¹⁴ which employs a plane-wave basis set and ultrasoft pseudopotentials.¹⁵ Downfolding to a three-band model containing copper $d_{x^2-y^2}$ and two oxygen p_σ orbitals was performed by the maximally localized Wannier functions (MLWF) method.^{16,17} We solve this model using dynamical mean-field theory with an exact impurity solver.¹⁸

We address the following questions: What are the spectral features that result from doping a charge-transfer insulator? How are these spectral features distributed in momentum space? How does the quasiparticle residue and the optical weight, induced by doping the charge-transfer insulator, vary with doping? We address the similarities and differences between our results and those that follow from a Hubbard model description.

Downfolding the LDA band structure of La_2CuO_4 results in the following three-band Hamiltonian:

$$\mathcal{H}_t = \sum_{ij\sigma, (\alpha,\beta) \in (p_x, p_y, d_{x^2-y^2})} t_{ij}^{\alpha\beta} c_{i\alpha\sigma}^\dagger c_{j\beta\sigma} + \epsilon_p \sum_{i\sigma\alpha \in (p_x, p_y)} \hat{n}_{i\alpha\sigma} + (\epsilon_d - E^{dc}) \sum_{i\sigma} \hat{n}_{id\sigma}, \quad (1)$$

where i and j label the CuO_2 unit cells of the lattice, and $t_{ij}^{\alpha\beta}$ are the hopping matrix elements. ϵ_d and ϵ_p are the on-site energies of the d and p orbitals, respectively.

The charge-transfer energy, Δ_{pd} , between the copper and oxygen plays the role of an effective onsite repulsion U in a Hubbard model picture, as seen for example in slave bosons mean-field studies.¹⁹

The LDA downfolding procedure results in $\epsilon_d - \epsilon_p = 2.78$ eV. To this Hamiltonian, we add the on-site Coulomb repulsion U on the $d_{x^2-y^2}$ orbital

$$\mathcal{H}_U = U_d \sum_i \hat{n}_{id\uparrow} \hat{n}_{id\downarrow}, \quad (2)$$

where the value of $U_d = 8$ eV. The LDA+DMFT method accounts for the correlations which are included in both LDA and DMFT by a double counting correction to the d -orbital energy, which we take to be fixed at $E_{dc} = 3.12$ eV for all dopings. We neglect the oxygen Coulomb repulsion U_p . Within single site DMFT, the copper-oxygen repulsion V_{dp} is treated at the Hartree level, and hence it is included in the orbital energies of the p and the d orbitals.

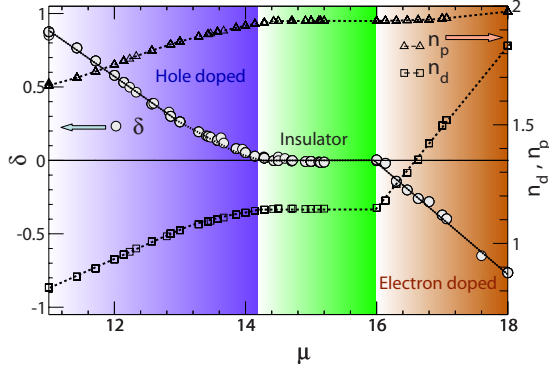


FIG. 1. (Color online) Doping δ (left scale) versus the chemical potential μ . The parent compound ($\delta=0$) is a charge-transfer insulator with a gap $\Delta_{pd} \approx 1.8$ eV (green region). The number of electrons in the $d_{x^2-y^2}$ orbital (n_d) and in the p_σ orbitals (n_p) is also shown (right scale).

The Green's function of the three-band model is given by

$$\mathbf{G}_k(i\omega_n) = [i\omega_n + \mu - \mathbf{H}_k - \mathbf{\Sigma}(i\omega_n)]^{-1}, \quad (3)$$

where \mathbf{H}_k is the Fourier transform of the \mathcal{H}_i in Eq. (1) and is a 3×3 matrix. $\mathbf{\Sigma}$ is the self-energy matrix being nonzero only in the d orbital.

The self-energy in Eq. (3) is obtained by solving an Anderson impurity model subject to the following DMFT self-consistency condition:

$$\frac{1}{i\omega - E_{\text{imp}} - \mathbf{\Sigma}(i\omega) - \Delta(i\omega)} = \frac{1}{N} \sum_{\mathbf{k} \in \text{BZ}} G_{\mathbf{k}}^{dd}(i\omega), \quad (4)$$

where the sum runs on the first Brillouin zone (BZ). In this work we use the continuous time quantum Monte Carlo (QMC) impurity solver algorithm,^{18,20} which gives the self-energy functional $\mathbf{\Sigma}[E_{\text{imp}}, \Delta]$ within the residual statistical error bars of the Monte Carlo algorithm.²¹ Real frequency resolved quantities were obtained by analytic continuation (more details will be given elsewhere²²) of the observables on the imaginary axis. We have cross-checked the analytic continuation using the OCA (noncrossing diagram approximation) real frequency solver.²³ Equations (1) and (2) were studied previously in Refs. 24 and 25. When U_d is large, there is a metal to charge-transfer insulator transition at integer filling, as a function of the charge-transfer energy $\epsilon_d - \epsilon_p$. For the set of realistic parameters considered in this paper, we find that the parent compound is a charge-transfer insulator (see Fig. 1), with a hole density per Cu atom $\approx 85\%$ and a charge gap close to 1.8 eV. This places this material slightly above (but not very far from) the metal to charge-transfer insulator transition point. This is demonstrated in Fig. 1, where the number of particles (δ) as a function of chemical potential (μ) exhibits a plateau in the interval $\mu = 14.2$ eV–16 eV. This figure also displays the partial occupancies, describing the relative distribution of the occupancies among copper and oxygen.

We have computed the spectral functions for both the parent and a doped compound. In the parent compound (not shown), we found four spectral peaks: (i) the upper Hubbard

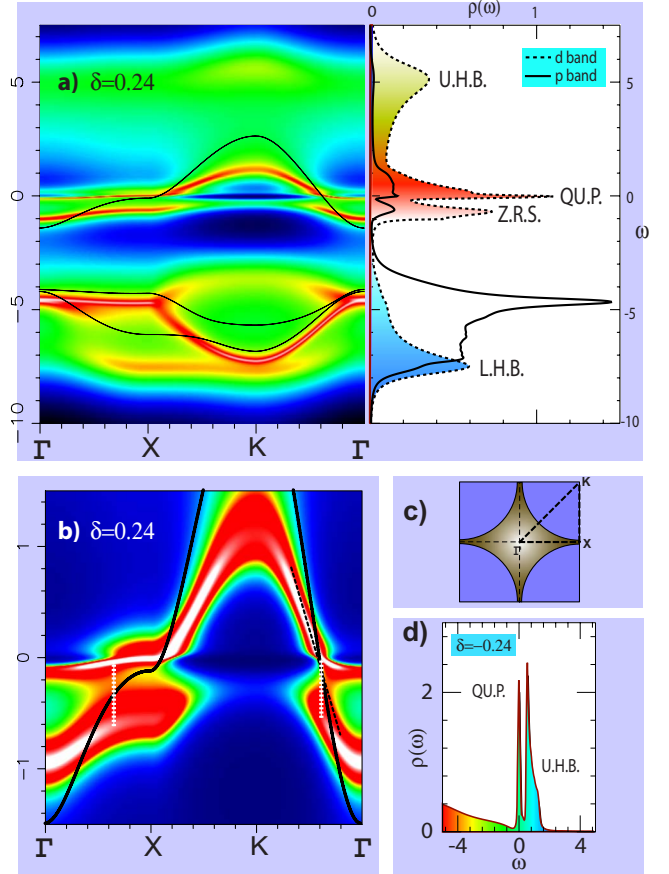


FIG. 2. (Color online) (a) Left panel: Spectral function $A(\mathbf{k}, \omega)$ for the hole-doped compound ($\delta=0.24$). The black lines correspond to the LDA bands. Right panel: The local spectral functions of the $d_{x^2-y^2}$ band (dashed line) and of the p_σ band (full line). We marked the positions of the lower Hubbard band (L.H.B.), coherent part of the Zhang-Rice singlet called the quasiparticle peak (Q.U.P.), the incoherent part of the Zhang-Rice singlet band (Z.R.S.) and the upper Hubbard band (U.H.B.). (b) The low energy part of $A(\mathbf{k}, \omega)$ from panel (a). The dashed line shows the slope of the quasiparticle band, which gives the Fermi velocity. The derivative was obtained by a quadratic expansion of $\mathbf{\Sigma}(\omega)$ at the Fermi level. The Fermi velocity in LDA+DMFT is $v_{\text{DMFT}}=2.15(5)$ Å eV in very favorable agreement with experiment [$v_{\text{exp}}=2.0$ Å eV at doping $\delta=0.24$ (Ref. 26)]. The ratio between the DMFT and the band velocity is thus $v_{\text{DMFT}}/v_{\text{LDA}}=0.49$. (c) Fermi surface and the path along which $A(\mathbf{k}, \omega)$ is shown in (a) and (b). (d) The density of states in the electron-doped compound. A very sharp quasiparticle peak develops close to the upper Hubbard band in the electron-doped case.

band around +2.5 eV, (ii) a singlet bound state of oxygen and copper known as the Zhang-Rice singlet just below the Fermi level, (iii) the oxygen set of bands centered around -7 eV, and (iv) the lower Hubbard band at -8 eV. By hole doping [see Fig. 2(a), right], the Zhang-Rice band is split into two peaks, the quasiparticle peak and the incoherent part which is associated with the lower Hubbard band in a single-band Hubbard model.

Figure 2(a) (left) and Fig. 2(b) show the momentum resolution of these features. The quasiparticle band crosses the Fermi level with a Fermi velocity along the nodal direction on the order of $v_{\text{Fermi}}=2.2$ Å eV in good agreement with

experimental results.²⁶ Figure 2(b) also shows a spectral gap around -0.3 eV, separating the coherent and incoherent parts of the Zhang-Rice band, with weak spectral weight connecting them. This is reminiscent of the waterfall feature observed in numerous cuprates. Moreover, our calculations lead to a very good agreement with experiments for both the range of energy where the high energy peak is present (≈ -1 eV) and the position in the Brillouin zone where the abrupt change is observed [close to $(\pi/2, \pi/2)$]. While there are many interpretations of this feature,²⁻⁶ we find that a proper description of the waterfall requires a multiband model containing both oxygen and copper orbitals, as pointed out in Ref. 4. The waterfall comes from the spectral gap between the incoherent part and the coherent (quasiparticle) part of the Zhang-Rice band.

Moreover, we emphasize that our calculations are quantitatively in very good agreement with experiments: we find that the waterfall ends up at the γ point at ≈ -1 eV, in very good agreement with spectroscopy experiments.^{2,3} Although the waterfall was also reported in one-band model studies,^{5,6} the many-band character of our calculations introduces some differences. In particular, we find some asymmetry between the correlated bands below and above the Fermi level. The lower correlated band has an incoherent character (incoherent part of the Zhang-Rice singlet), whereas the upper band is very coherent (quasiparticle peak). Moreover, the correlated bands obtained by one-band model calculations are mainly following the bare band structure. We catch some more subtle effects of the correlations in our calculations that introduce some additional modifications of the correlated band structure, which has clearly a different structure as the LDA bands.

Moreover, the waterfall is not present in the single site DMFT description of the parent compound, and our calculation in paramagnetic state of La_2CuO_4 does not show splitting of the Zhang-Rice band into a low energy and a high energy part. We have found, however, that when the antiferromagnetic broken symmetry state is considered for a parent compound, the splitting of the Zhang-Rice singlet is present, and the low energy part of the Zhang-Rice band is touching the Fermi level at $(\pi/2, \pi/2)$ momentum.

One of the most notable aspects of cuprate physics is the rapid growth of the optical conductivity inside the charge gap upon hole doping.²⁷ This latter effect was noted early on by Eskes *et al.*²⁸ and reported more recently by Tohyama *et al.*²⁹ in an exact diagonalization study of the one-band model.

In order to tackle this issue, we computed the optical conductivity given by

$$\sigma'(\omega) = \frac{1}{N_k} \sum_{\sigma\mathbf{k}} \frac{\pi e^2}{\hbar c} \int dx \frac{f(x-\omega) - f(x)}{\omega} \times \text{Tr}[\hat{\rho}_{\mathbf{k}\sigma}(x-\omega) \mathbf{v}_{\mathbf{k}} \hat{\rho}_{\mathbf{k}\sigma}(x) \mathbf{v}_{\mathbf{k}}], \quad (5)$$

where c is the interlayer distance, the density matrix $\hat{\rho}$ is defined by

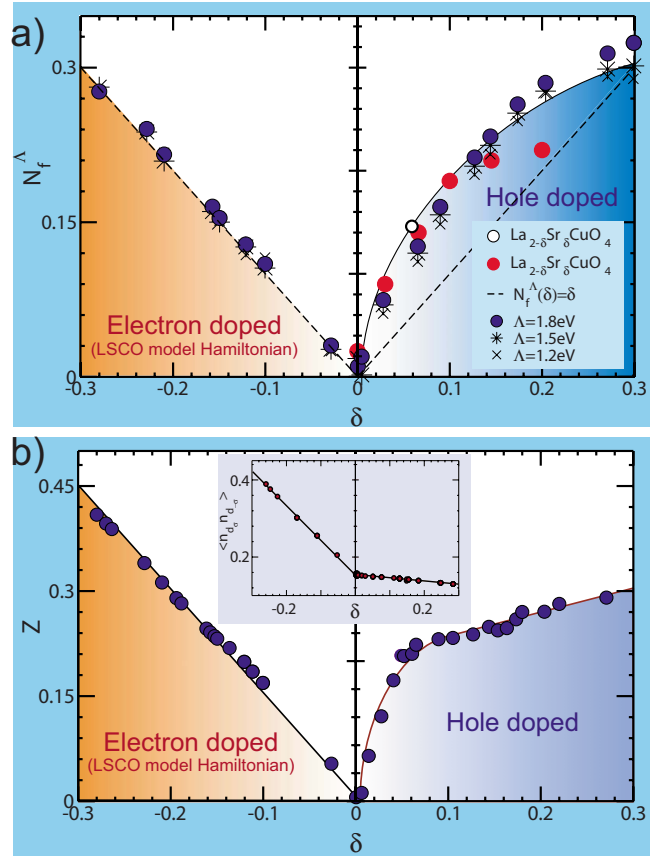


FIG. 3. (Color online) Optical conductivity $\sigma(\omega)$ for the parent compound ($\delta=0$) and the hole-doped compound ($\delta=0.24$). For the parent compound, we show optics in the Neel state. The optical gap in the parent compound is around 1.8 eV in both the paramagnetic and antiferromagnetic state. The structure around $\omega=8$ eV corresponds to transitions between the lower and the upper Hubbard band. Upon hole doping, an additional peak appears close to $\omega \approx 1$ eV for a large range of doping ($\delta=5-30\%$). It corresponds to transitions between the quasiparticle part and incoherent part of the Zhang-Rice singlet.

$$\hat{\rho}_{\mathbf{k}\sigma}(x) = \frac{1}{2\pi i} [\mathbf{G}_{\mathbf{k}\sigma}^\dagger(x) - \mathbf{G}_{\mathbf{k}\sigma}(x)], \quad (6)$$

and the bare vertex is given by $\mathbf{v}_{\mathbf{k}} = d\hat{\mathbf{H}}_{\mathbf{k}}/dk_x$. Our results are displayed in Fig. 3. The optical gap in the parent compound is found to be 1.8 eV. To quantify the rate of the redistribution of optical spectral weight, we computed the effective electron number per Cu atom defined by

$$N_{\text{eff}}^\Lambda = \frac{2m_e V}{\hbar \pi e^2} \int_0^\Lambda \sigma'(\omega) d\omega, \quad (7)$$

where m_e is the free electron mass, and V is the cell volume containing one formula unit. N_{eff} is proportional to the number of electrons involved in the optical excitations up to the cutoff Λ . Our results for N_{eff} are displayed in Fig. 4 and compared to experimental data taken from Ref. 27.

We emphasize that the agreement between our calculations and the experimental data at the quantitative level is

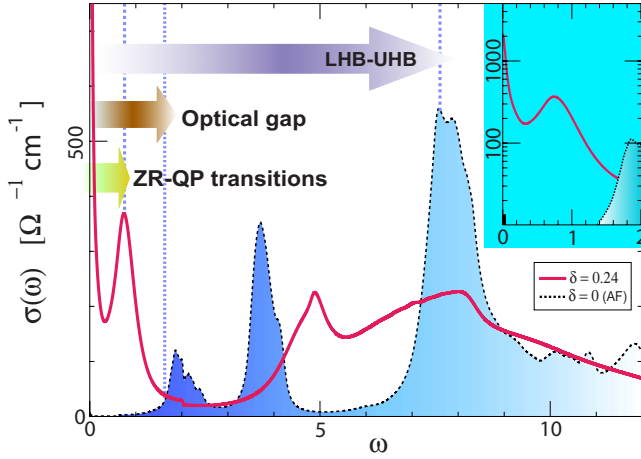


FIG. 4. (Color online) (a) Optical spectral weight N_{eff} obtained by Eq. (7) using various cutoffs $\Lambda=1.2, 1.5, 1.8$ eV for both the hole doping ($\delta>0$) and electron doping ($\delta<0$). The experimental data (red circles) are reproduced from Ref. 27. The long dashed line corresponds to the curve $N_{\text{eff}}(\delta)=\delta$. Note the asymmetry between the electron ($\delta<0$) and hole-doped ($\delta>0$) side. For completeness, we also present more recent experimental data obtained by infrared spectroscopy of LSCO (white circle). The data are reproduced from Ref. 30. (b) The quasiparticle weight Z versus doping. Inset: double occupancy of the $d_{x^2-y^2}$ orbital versus doping. For the electron-doped compound, the double occupancy increases linearly with doping, whereas the hole doping has only a weak effect on double occupancy of the $d_{x^2-y^2}$ orbital. The continuous lines are guides for the eyes.

remarkable. It confirms clearly the validity of our approach to describe the optical properties of hole-doped compounds (LSCO).

Notice that the spectral weight, contained in the region below the charge-transfer gap of the parent compound, grows in a superlinear fashion. This is in agreement with experiments of Ref. 27 but is incompatible within a rigid band picture of doping either a band or a Mott insulator far from the Mott transition (as for example in the Hubbard model well above U_{c2} , where U_{c2} is commonly defined as the critical Coulomb repulsion necessary to open a gap for the paramagnetic state). Thus the optical spectral weight in the charge-transfer insulator grows faster with doping than in the Mott insulator, where the linear growth of the spectral weight is expected.

The realistic three-band model within single site DMFT approach leads to a considerable asymmetry in the electron and hole-doped side of the phase diagram. The superlinear behavior found in our calculation of the three-band model is sufficient to explain the experimental findings, even though the correlations are strong enough to open a charge-transfer gap in the parent compound even in the paramagnetic state.

We verified that this interesting particle hole asymmetry is present also in the quasiparticle residue $Z=(1-\frac{d\Sigma'(\omega)}{d\omega})^{-1}$ and

is shown in Fig. 4(b). This is a one-electron quantity that can be obtained directly from the imaginary axis data without the need to invoke analytic continuation but still follows the same trend as N_{eff} .

It is interesting to compare the asymmetry found here with the recent results of Ref. 31 on the Anderson lattice model. The authors found a much larger particle hole asymmetry compared to our results. Most likely this is due to a momentum-independent hybridization function, which makes the Kondo scale in the hole-doped side very small,³² and hard to reach with conventional QMC.

Phenomena in the underdoped region, such as the normal state pseudogap and the formation of Fermi arcs, are not described by single site DMFT and require cluster extensions of the formalism.³³ However, single site DMFT is still expected to describe well intermediate energy phenomena, such as the distribution of the spectral weight upon doping the Mott/charge transfer insulator, which is the focus of our work. Momentum resolved quantities become more accurate in the overdoped region, where the self-energy is more local.

For this reason, we have not considered here the details of the momentum-dependent photoemission spectra at low doping, or the details of the frequency-dependent optical conductivity, which are considerably influenced by cluster effects. We have rather focused on quantities such as N_{eff} , which are less sensitive to cluster corrections and rather presented the detailed photoemission spectra in the overdoped region, where actually the local approximation is valid.³³

In conclusion, we have carried out a realistic LDA+DMFT calculation accounting for the $d_{x^2-y^2}$ and p_{σ} orbitals of the three-band model. The electron-doped side is behaving mainly like the single-band Hubbard model. On the other hand, the hole-doped side of the phase diagram is very different. (a) We find a superlinear optical spectral weight transfer in agreement with experiments. (b) On the spectral function, we find a spectral gap between the quasiparticle band and the incoherent Zhang-Rice singlet band. This leads to a very abrupt and nearly vertical change in the spectral intensity in the nodal direction of the spectrum (*waterfall*) that ends up below 1 eV.

Our LDA+DMFT study supports the view that the hole-doped cuprates are above but not very far from the metal charge-transfer insulator transition in agreement with the conclusion of earlier slave boson studies.¹⁹ It would be interesting to apply further the same methodology to the electron-doped cuprates, which have a smaller charge-transfer gap. These materials might have a charge-transfer energy which lies below or much closer to the critical value needed to sustain a paramagnetic insulator at integer filling, and hence might undergo a different metallization process upon doping, as suggested in Ref. 34.

We thank C. A. Marianetti, L. de' Medici, M. Ferrero, and C. Varma for many illuminating discussions. C.W. and G.K. were supported by NSF under Grant No. DMR 0528969.

- ¹A. Comanac, L. de' Medici, M. Capone, and A. J. Millis, *Nat. Phys.* **4**, 287 (2008).
- ²T. Valla, T. E. Kidd, W.-G. Yin, G. D. Gu, P. D. Johnson, Z.-H. Pan, and A. V. Fedorov, *Phys. Rev. Lett.* **98**, 167003 (2007).
- ³D. S. Inosov, J. Fink, A. A. Kordyuk, S. V. Borisenko, V. B. Zabolotnyy, R. Schuster, M. Knupfer, B. Büchner, R. Follath, H. A. Dürr, W. Eberhardt, V. Hinkov, B. Keimer, and H. Berger, *Phys. Rev. Lett.* **99**, 237002 (2007).
- ⁴Q. Yin, A. Gordienko, X. Wan, and S. Y. Savrasov, *Phys. Rev. Lett.* **100**, 066406 (2008).
- ⁵A. Macridin, M. Jarrell, T. Maier, and D. J. Scalapino, *Phys. Rev. Lett.* **99**, 237001 (2007).
- ⁶M. M. Zemljič, P. Prelovšek, and T. Tohyama, *Phys. Rev. Lett.* **100**, 036402 (2008).
- ⁷G. A. Sawatzky and J. W. Allen, *Phys. Rev. Lett.* **53**, 2339 (1984).
- ⁸J. Zaanen, G. A. Sawatzky, and J. W. Allen, *Phys. Rev. Lett.* **55**, 418 (1985).
- ⁹V. J. Emery, *Phys. Rev. Lett.* **58**, 2794 (1987).
- ¹⁰C. M. Varma, S. Schmitt-Rink, and E. Abrahams, *Solid State Commun.* **62**, 681 (1987).
- ¹¹G. Dopf, A. Muramatsu, and W. Hanke, *Phys. Rev. Lett.* **68**, 353 (1992).
- ¹²F. C. Zhang and T. M. Rice, *Phys. Rev. B* **37**, 3759 (1988).
- ¹³G. Kotliar, S. Y. Savrasov, K. Haule, V. S. Oudovenko, O. Parcollet, and C. A. Marianetti, *Rev. Mod. Phys.* **78**, 865 (2006).
- ¹⁴S. Baroni, S. de Gironcoli, A. Dal Corso, and P. Giannozzi, *PWSCF in Quantum Espresso Package*, 2007, <http://www.pwscf.org/>
- ¹⁵D. Vanderbilt, *Phys. Rev. B* **41**, 7892 (1990).
- ¹⁶I. Souza, N. Marzari, and D. Vanderbilt, *Phys. Rev. B* **65**, 035109 (2001).
- ¹⁷A. A. Mostofi, J. R. Yates, Y.-S. Lee, I. Souza, D. Vanderbilt, and N. Marzari, *Comput. Phys. Commun.* **178**, 685 (2008).
- ¹⁸K. Haule, *Phys. Rev. B* **75**, 155113 (2007).
- ¹⁹G. Kotliar, *Int. J. Mod. Phys. B* **5**, 341 (1991).
- ²⁰P. Werner, A. Comanac, L. de' Medici, M. Troyer, and A. J. Millis, *Phys. Rev. Lett.* **97**, 076405 (2006).
- ²¹In this work we used temperature $T=116$ K.
- ²²K. Haule and C. Weber (unpublished).
- ²³K. Haule, S. Kirchner, J. Kroha, and P. Wölfle, *Phys. Rev. B* **64**, 155111 (2001).
- ²⁴A. Georges, Gabriel Kotliar, and W. Krauth, *Z. Phys. B: Condens. Matter* **92**, 313 (1993).
- ²⁵P. Lombardo, J. Schmalian, M. Avignon, and K.-H. Bennemann, *Phys. Rev. B* **54**, 5317 (1996).
- ²⁶X. J. Zhou, T. Yoshida, A. Lanzara, P. V. Bogdanov, S. A. Kellar, K. M. Shen, W. L. Yang, F. Ronning, T. Sasagawa, T. Kakeshita, T. Noda, H. Eisaki, S. Uchida, C. T. Lin, F. Zhou, J. W. Xiong, W. X. Ti, Z. X. Zhao, A. Fujimori, Z. Hussain, and Z.-X. Shen, *Nature (London)* **423**, 398 (2003).
- ²⁷S. Uchida, T. Ido, H. Takagi, T. Arima, Y. Tokura, and S. Tajima, *Phys. Rev. B* **43**, 7942 (1991).
- ²⁸H. Eskes, M. B. J. Meinders, and G. A. Sawatzky, *Phys. Rev. Lett.* **67**, 1035 (1991).
- ²⁹T. Tohyama, Y. Inoue, K. Tsutsui, and S. Maekawa, *Phys. Rev. B* **72**, 045113 (2005).
- ³⁰M. Dumm, S. Komiyama, Y. Ando, and D. N. Basov, *Phys. Rev. Lett.* **91**, 077004 (2003).
- ³¹G. Sordi, A. Amaricci, and M. J. Rozenberg, *Phys. Rev. Lett.* **99**, 196403 (2007).
- ³²M. Grilli, B. G. Kotliar, and A. J. Millis, *Phys. Rev. B* **42**, 329 (1990).
- ³³K. Haule and G. Kotliar, *Phys. Rev. B* **76**, 104509 (2007).
- ³⁴D. Sénéchal and A.-M. S. Tremblay, *Phys. Rev. Lett.* **92**, 126401 (2004).